Graphene

Photocurrent Distribution in Graphene–CdS Nanowire Devices

Thomas Dufaux, Jens Boettcher, Marko Burghard, and Klaus Kern*

In order to realize solar cells with technologically useful performance, intensive efforts are being directed towards the development of novel device architectures and components. So far, high power conversion efficiencies exceeding 5% have been reached with dye-sensitized[1] or polymer blend-based solar cells,[2] wherein very fast interfacial charge transfer occurs. However, charge transport is often limiting the performance of these devices. In particular for blend-based solar cells, the photocurrent depends strongly on the properties of the percolation network.[3] A promising strategy to overcome this limitation involves nano-structured solar cells which provide well-defined, separate pathways for carrier transport, thus minimizing recombination losses. Examples include vertically aligned arrays of ZnO,[4] TiO_2,[5] Si nanowires,[6] or TiO_2 functionalized CNTs.[7] Especially promising are CNTs decorated with semiconductor nanoparticles, since the former provide a close-to-ideal transport pathway for carriers. However, it is difficult to obtain a high quality electrical connection between nanotube and semiconductor without disrupting the carbon framework of the nanotubes. Accordingly, studying the interface between sp^2-bonded carbon materials and semiconductors is important for further improving the performance of CNT based solar cells. More recently, also the closely related graphene has attracted increasing interest toward photovoltaic applications.[8] It has been chemically modified by the attachment of TiO_2 nanoparticles[9] or CdS quantum dots,[10] albeit only little is known about the interface between graphene and inorganic or organic semiconductors, in contrast to the metal–graphene interaction.[11–13] In fact, while ultrafast electron transfer from CdS dots to graphene has been detected by time-resolved photoluminescence spectroscopy,[14] the suitability of these nanocomposites for light harvesting applications remains to be evaluated.

Here, we investigate the photoelectric properties of the interface between graphene as a carbon nanostructure and CdS as a widely used II–VI semiconductor. In this model system, the graphene sheet is contacted with a CdS nanowire which serves to transport electrons to the opposite metal contact. The lateral device configuration allows scanning photocurrent microscopy (SPCM) to be used to map the generated photocurrents with sub-micrometer resolution. In contrast to bulk solar cells, this opens the possibility to distinguish between photoresponses of the involved interfaces at the nanoscale. Although due to the ultrasmall photoactive interfacial area in these devices, they naturally exhibit only low photoconversion efficiencies, they provide a valuable platform to explore strategies for chemical interface tailoring.

The final device structure is illustrated by the atomic force microscopy (AFM), optical microscopy and optical reflection images in **Figure 1**a. In this device, the contacted graphene consists of a narrow (~0.3 μm width) and a wide (~1.2 μm width) stripe that are arranged in parallel and connected through the remaining sheet. Under dark conditions, the devices generally did not exhibit any measurable current between the gold and titanium contacts. To study the effect of local illumination, the devices were scanned through the diffraction-limited laser spot of a confocal microscope. These SPCM experiments[15,16] were performed under ambient conditions. A reflection image and a photocurrent map were recorded simultaneously, allowing the assignment of features in the photocurrent map to the sample structure. In all samples, the titanium contact was connected as source, and the AuPd electrode as drain. The SPCM image of the aforementioned device (Figure 1b), displays pronounced photocurrent signals on the order of –0.7 nA at the two intersections between the CdS nanowire (~50 nm diameter, as determined from the AFM section profile) and the edges of the underlying wider graphene stripe (AFM thickness ~2 nm). By contrast, the edge signals have merged into one signal in case of the narrower stripe. A similar signal pattern has been observed in six other samples. Among these, only two displayed a very weak response along the entire interface. All measurements were performed at λ_{exc} = 488 nm. At higher wavelength only very low photopresponses could be observed since the excitation was below the bandgap of the CdS.

The photocurrent response reflects the presence of potential barriers in the CdS wire, and its negative sign indicates that the local built-in electric field drives the photogenerated electrons along the CdS wire to the Ti contact, whereas the holes are injected into the graphene sheet from where they travel to the AuPd contact. It thus follows that upon contact formation between the two materials, electrons are transferred from the

T. Dufaux, Dr. J. Boettcher, Dr. M. Burghard, Prof. K. Kern
Max-Planck-Institut fuer Festkoerperforschung
Heisenbergstrasse 1, 70569 Stuttgart, Germany
E-mail: T.Dufaux@fkf.mpg.de
Prof. K. Kern
Institute de Physique de la Matière Condensée
Ecole Polytechnique de Lausanne
1015 Lausanne, Switzerland

DOI: 10.1002/smll.201000950

small NANO MICRO

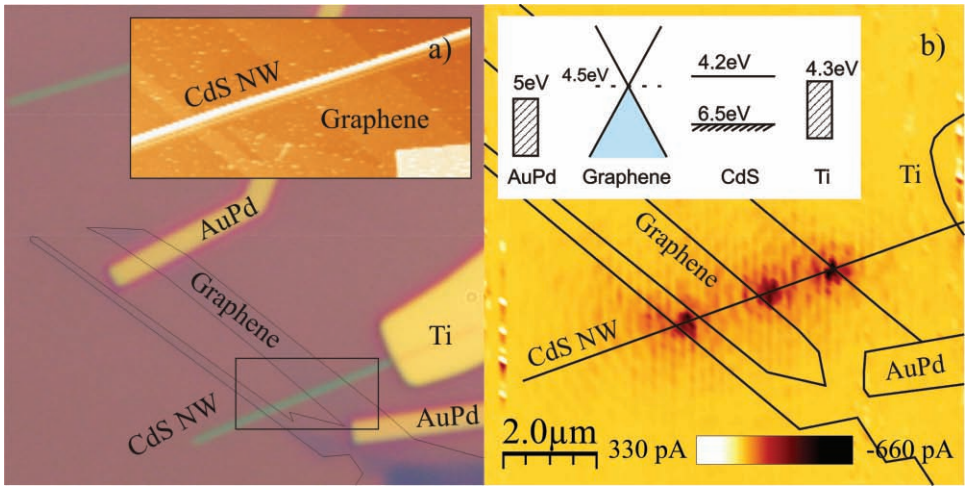

Figure 1. a) Optical image of a nanoscale graphene–CdS nanowire solar cell. The inset shows an AFM image of the graphene/CdS interface. b) Zero-bias SPCM image of a graphene–CdS nanowire device, revealing a photoresponse at the intersection of the graphene edge and the wire. The three major lobes are surrounded by concentric features which originate from diffraction of the focused laser beam. The inset represents an energy diagram of the device components.

CdS nanowire to graphene, which leads to an upward band bending within the wire section close to the graphene interface. On this basis, it can be concluded that the CdS wires are n-doped to such an extent that their work function is below that of graphene (~4.5 eV[13]). This doping could be due to the introduction of sulfur vacancies on CdS wires as it was shown in previous studies.[17] The finding that the photoresponse is strongly localized at the edge of the graphene sheet, instead of being distributed homogeneously along the entire CdS–graphene interface, can be partially ascribed to the presence of adsorbates on the graphene sheet, which can be removed by annealing (see below).

Another noteworthy observation is the lack of a photoresponse at the Ti–CdS nanowire and AuPd–graphene contacts in the photocurrent map. The same behavior has been observed for several other graphene–CdS nanowire devices. A plausible explanation for the negligible signal at the Ti–CdS contact is the lower work function of titanium (4.3 eV[18,19]) in comparison to graphene, which enables the formation of a quasi-ohmic contact, in close correspondence to observations made on Ti-contacted individual CdS nanoribbons.[20] Upon illumination of the AuPd–graphene interface, a flow of holes would be expected toward the metal contact due to the local potential step.[8] The absence of such signal is attributable to the electron transport barrier that exists at the graphene–CdS interface. This barrier also contributes to the very high device resistance in the dark.

The weak, varying and inhomogeneous photocurrents are indicative of a non-intimate contact between graphene and the CdS wire. It could be significantly improved via chemical control of the graphene–CdS interface (**Figure 2**a). To this end, the CdS wires were first dispersed in dilute aqueous HCl (pH 2) in order to remove the CdO layer from their surface. Subsequently, thioglycerol HS-CH_2-CH(OH)-CH_2-OH was added (10 μL per 10 mL) as a ligand capable of stabilizing the CdS surface via covalent attachment.[21] After removal of the excess thiol by several consecutive centrifugation and washing steps, the surface-capped CdS wires were deposited onto the graphene-coated substrate. Finally, an annealing step (15 min at 350 °C under argon) was performed with the aim of removing the ligand on the CdS wire as well as adsorbates on the graphene sheet. These adsorbates are probably leftovers of the e-beam resist[22] combined with water adsorbed from the ambient.[23] The resulting improved contact between graphene and the CdS wire is manifested by two major changes in comparison to the above described devices, as can be discerned from the SPCM image in Figure 2b. Firstly, the devices displayed considerably larger short-circuit photocurrents, which reached up to 200 nA for strongest laser intensity (191 kW cm^{-2}), corresponding to an enhancement by approximately two orders of magnitude. Secondly, the photoresponse is no longer restricted to the intersection between sheet edge and wire, but rather distributed along the entire graphene–CdS interface. The creation of an intimate graphene–CdS interface during annealing is likely caused by coordinative bond formation between the Cd^{2+} ions on the CdS surface and the π-conjugated electrons in graphene, akin to the interaction between graphene and CdSe nanoparticles attached via solution-based process.[24] It should be noted that also annealing alone, i.e., without prior CdO removal and CdS surface capping, resulted in a notable photocurrent increase, albeit the enhancement was limited to a factor of only 10. This finding illustrates that the removal of contaminants on the graphene sheet contributes to the better electronic coupling between the two materials. Adsorbates on graphene are known to impede the charge carrier transport in graphene, making for example Joule heating necessary in order to remove these scattering centers and thus reach high electrical performance.[25] The samples could be stored for several weeks under ambient conditions without any observable degradation of the device performance. Figure 2c shows the linear dependence of the short circuit current as a function of the illumination intensity.

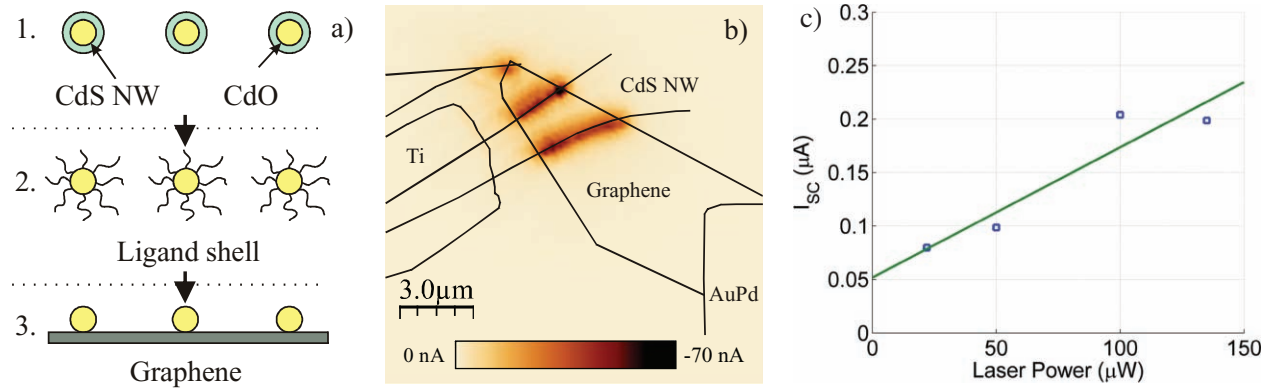

Figure 2. a) Scheme illustrating the chemical modification steps used to improve the coupling between a CdS nanowire and the underlying graphene. The steps comprise 1) the removal of CdO from the CdS wire surface by dilute aqueous acid, 2) addition of thioglycerol as a capping ligand, and finally 3) annealing to simultaneously remove the ligands and adsorbates on the graphene surface. b) A zero-bias photocurrent map of a graphene–CdS nanowire device subjected to the steps described in panel a. In contrast to unmodified devices, a strong photoresponse emerges along the entire graphene–CdS interface. c) The short-circuit current as a function of the illumination intensity. The green line is a linear fit of the data points.

Figure 3a presents *I–V* curves of a CdS–graphene contact before and after interface improvement. As the devices are insulating in the dark, the generated photocurrents can be entirely attributed to separated electron–hole pairs. With increasing negative bias the photocurrent rises owing to the enhanced separation of electron-hole pairs in the stronger electric field. Moreover, under forward bias there emerges a positive photocurrent, which likely originates from weak co-illumination of the Ti/CdS interface (see discussion below). The considerable photocurrent increase after interface improvement is accompanied by a decrease of the open-circuit voltage from 0.17 V to less than 0.1 V, pointing toward an increased recombination rate. The latter change causes a drop of the fill factor (FF) from 35% to 23%, which falls significantly below those reported for dye-sensitized solar cells (FF up to 75%),[26] but nonetheless compares favorably to graphene-based bulk heterojunction cells.[27] The absolute photocurrents collected from the present single-interface devices are inherently much lower than the currents in bulk solar cells. Downscaling the typical bulk photocurrents of the order of 1 mA cm^{-2} to a single interface with an illuminated area of 0.07 μm^2 (corresponding to the size of the confocal laser spot) would yield a current of 0.7 pA, well below the 200 nA measured in our devices. This difference results from the high illumination intensities in the SPCM experiments.

The internal power conversion efficiency (IPCE) can be obtained from

$$\eta = \frac{V_{OC} \cdot I_{SC} \cdot FF}{P_{in} \cdot \alpha}$$

where V_{OC} is the open circuit voltage, I_{SC} the short circuit current, FF the fill factor, P_{in} the light intensity, and α represents the fraction of absorbed light. A low value of $\alpha = 0.01$ was calculated by finite-difference time-domain (FDTD) simulations using Meep[28] (see ref.[29] for the optical constants of CdS). In contrast to bulk solar cells, re-absorption and light scattering, which would increase the length of the light path, play only a minor role in the present devices. Thus the amount of absorbed light is much lower, leading to a low α. Despite the small absorption, the IPCE remains small at 0.34% as a consequence of the aforementioned high recombination rate. It is noteworthy that by inserting a hole blocking layer such as TiO_2, the recombination and accordingly the IPCE might be improved, analogous to vertical carbon nanotube arrays sensitized by TiO_2.[5]

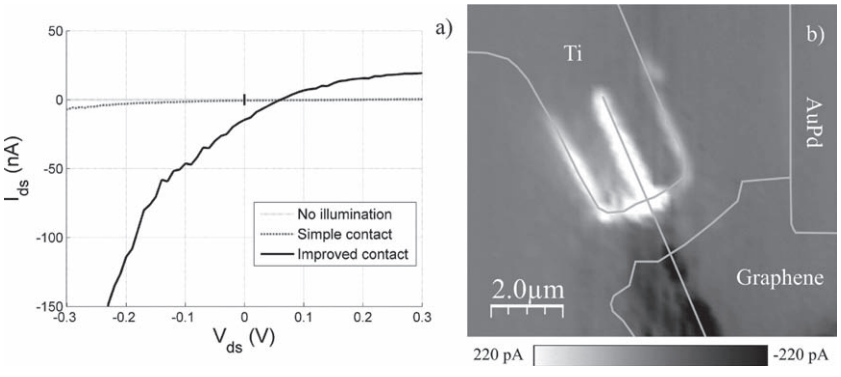

Figure 3. a) Current–voltage characteristics of a graphene–CdS nanowire device recorded under ambient in the dark (blue curve), without (green curve) and with (red curve) interface improvement. The laser spot (λ_{exc} = 488 nm) was positioned at the maximum current of the SPCM map. b) Zero-bias photocurrent map of a graphene–CdS nanowire device modified using the protocol in Figure 2a. Besides the photoresponse at the graphene–CdS interface (black signal at the bottom), an additional signal (white) can be seen at Ti–CdS interface and along the edges of the Ti electrode. The latter feature is ascribed to the creation of electron–hole pairs at the Ti–CdS interface by surface plasmons originating from the Ti electrode edge.

The devices comprising an improved CdS–graphene interface exhibited two further novel features, which can be discerned in the SPCM image of Figure 3b. The first

small NANO MICRO

one is the emergence of a photoresponse at the Ti contact to the CdS nanowire, whose positive sign signifies that holes are transferred from the CdS to titanium, corresponding to a current direction opposite to the built-in electric field implemented by the work function difference between the Ti and AuPd contact. On this basis, it can be concluded that strong n-doping of the CdS wires has occurred during the argon plasma and surface chemical treatment, such that the work function of CdS is reduced below that of titanium. Pronounced n-doping of the CdS surface may arise from thermally induced removal of sulfur, analogous to the effect of annealing on pyridine-capped CdSe nanocrystals.[30]

As the second novel feature, photocurrent signals occur along the CdS nanowire underneath the electrode, as well as along the edges of the titanium contact, where they extend up to the projection of the nanowire tip in this direction. We attribute them to the excitation of surface plasmons at the Ti electrode edge, which then propagate along the Ti–SiO_2 and Ti–air interfaces to the Ti–CdS contact. The possibility of electron-hole pair excitation in semiconductor nanowires by the electric near field associated with surface plasmons in a closely attached metallic nanostructure has recently been documented.[31] In the present case, the sharp electrode edges represent a single line of a grating, which in k-space allows coupling to numerous plasmons modes.[32] Surface plasmon modes can propagate in titanium for wavelengths above $\lambda_{\mathrm{Ti,SPP}} = 140$ nm, as estimated from $E_{SPP} = h\sqrt{\frac{2ne^2}{m\varepsilon_0}}$.[33] Further support for the surface plasmon mechanism derives from the decay length L defined as $L = 1/(2k_{x,Ti})$, where $k_{x,Ti}$ is the imaginary part of the wavevector of a propagating surface plasmon, which can be calculated from the SPP dispersion relation[34] according to

$$k_{x,Ti} = k_0\sqrt{\frac{\varepsilon_{Ti}\varepsilon_{air}}{\varepsilon_{Ti} + \varepsilon_{air}}}$$

Solving this equation yields a decay length of ~1 μm, a value similar to the distance between long edges of the Ti contact and the CdS wire. Correspondingly, more remote edge sections cannot contribute to the signal, as plasmons generated at these locations are too strongly attenuated before reaching the Ti–CdS interface.

In summary, we successfully demonstrated the use of SPCM in the study of planar, nanostructured solar cells comprising a graphene–CdS contact. The detailed knowledge of the photocurrents generated at each of the involved interfaces provides a suitable basis for optimizing their electronic properties, and correspondingly the overall photoconversion efficiency. Thus, future SPCM studies on similar types of nanoscale devices could help indentifying strategies to tailor the energy landscape in these devices through appropriate interface engineering.

Experimental Section

For fabricating the graphene–CdS nanowire devices, first graphene sheets were mechanically exfoliated from highly oriented pyrolytic graphite (HOPG) and transferred on Si substrates with a 300 nm thick thermally grown SiO_2 layer. Single- or multilayered sheets were located using optical microscopy. The CdS nanowires were synthesized by a solvothermal method using cadmium diethyldithiocarbamate $[Cd(S_2CN(CH_2CH_3)_2]_2$ as precursor and ethylenediamine $H_2N\text{-}CH_2\text{-}CH_2\text{-}NH_2$ as coordinating solvent.[35] After 48 h of growth at 200 °C, single-crystalline CdS wires with lengths of up to 20 μm and diameters in the range of 20 to 80 nm were obtained. The wires were dispersed in ethanol with the aid of ultrasonication, and subsequently deposited onto the graphene covered substrates through several spin coating steps, each employing 20 μL droplets at 5000 rpm. Afterwards, electrical contacts to the graphene and the CdS nanowires were defined by e-beam lithography. In case of the CdS nanowires, the exposed segments were treated by an Ar-plasma,[36,37] immediately followed by evaporation of 90 nm of titanium. The Ar-plasma is necessary to n-dope the nanowire surface prior to the evaporation of Ti.[38] The contacts to the graphene sheets were made by 90 nm of AuPd (60/40) with a ~0.8 nm Ti adhesion layer.

Acknowledgements

This work was supported by the Bundesministerium für Bildung und Forschung (BMBF) within the framework of the SONAPOLY project. The authors thank A. Sagar and B. Krauss for experimental support, as well as D. Kälblein, J. Dorfmueller and R. Vogelgesang for valuable discussions.

[1] B. Oregan, M. Gratzel, *Nature* **1991**, *353*, 737.
[2] X. Yang, J. Loos, S. C. Veenstra, W. J. H. Verhees, M. M. Wienk, J. M. Kroon, M. Michels, R. Janssen, *Nano Lett.* **2005**, *5*, 579.
[3] W. U. Huynh, J. J. Dittmer, A. P. Alivisatos, *Science* **2002**, *295*, 2425.
[4] J. B. Baxter, E. S. Aydil, *Appl. Phys. Lett.* **2005**, *86*, 053114.
[5] G. K. Mor, K. Shankar, M. Paulose, O. K. Varghese, C. A. Grimes, *Nano Lett.* **2006**, *6*, 215.
[6] A. P. Goodey, S. M. Eichfeld, K. K. Lew, J. M. Redwing, T. E. Mallouk, *J. Am. Chem. Soc.* **2007**, *129*, 12344.
[7] J. Liu, Y. T. Kuo, K. J. Klabunde, C. Rochford, J. Wu, J. Li, *Appl. Mat. Int.* **2009**, *8*, 1645.
[8] Z. Liu, Q. Liu, Y. Huang, Y. Ma, S. Yin, X. Zhang, W. Sun, Y. Chen, *Adv. Mater.* **2009**, *20*, 3924.
[9] G. Williams, B. Seger, P. V. Kamat, *ACS Nano* **2008**, *2*, 1487.
[10] A. Cao, Z. Liu, S. Chu, M. Wu, Z. Ye, Z. Cai, Y. Chang, S. Wang, Q. Gong, Y. Liu, *Adv. Mater.* **2009**, *21*, 1.
[11] E. J. H. Lee, K. Balasubramanian, R. T. Weitz, M. Burghard, K. Kern, *Nature Nanotechnol.* **2008**, *3*, 486.
[12] Y. M. Blanter, I. Martin, *Phys. Rev. B* **2007**, *76*, 155433.
[13] G. Giovannetti, P. A. Khomyakov, G. Brocks, V. M. Karpan, J. Van Den Brink, P. J. Kelly, *Phys. Rev. Lett.* **2008**, *101*, 026803.
[14] T. Gao, Q. H. Li, T. H. Wang, *Appl. Phys. Lett.* **2005**, *86*, 173105.
[15] Y. Ahn, J. Dunning, J. Park, *Nano Lett.* **2005**, *5*, 1367.
[16] D. V. Lang, C. H. Henry, *Solid-State Electron.* **1978**, *21*, 1519.
[17] S. Kitamaru, *J. Phys. Soc. Jpn.* **1960**, *15*, 12.
[18] R. J. Darcy, N. A. Surplice, *Surf. Sci.* **1973**, *36*, 783.
[19] *CRC Handbook of Chemistry and Physics* (Ed: D. R. Lide), CRC Press, Boca Raton, FL **2008**.
[20] J. S. Jie, W. J. Zhang, Y. Jiang, X. M. Meng, Y. Q. Li, S. T. Lee, *Nano Lett.* **2006**, *6*, 1887.
[21] H. Doellefeld, K. Hoppe, J. Kolny, K. Schilling, H. Weller, A. Eychmueller, *Phys. Chem. Chem. Phys* **2002**, *4*, 4747.

[22] M. Ishigami, J. H. Chen, W. G. Cullen, M. S. Fuhrer, E. D. Williams, *ACS Nano* **2007**, *7*, 1643.
[23] T. O. Wehling, K. S. Novoselov, S. V. Morozov, E. E. Vdovin, M. I. Katsnelson, A. K. Geim, A. I. Lichtenstein, *ACS Nano* **2008**, *8*, 173.
[24] B. H. Juarez, M. Meyns, A. Chanaewa, Y. X. Cai, C. Klinke, H. Weller, *J. Am. Chem. Soc.* **2008**, *130*, 15282.
[25] J. Moser, A. Barreiro, A. Bachtold, *Appl. Phys. Lett.* **2007**, *91*, 163513.
[26] D. Shi, Y. P. N. Cao, *J. Phys. Chem. C* **2008**, *112*, 17478.
[27] Q. Liu, Z. Liu, X. Zhang, L. Yang, N. Zhang, G. Pan, S. Yin, Y. Chen, J. Wei, *Adv. Funct. Mater.* **2009**, *19*, 894.
[28] A. F. Oskooi, D. Roundy, M. Ibanescu, P. Bermel, J. D. Joannopoulos, S. G. Johnson, *Comput. Phys. Commun.* **2010**, *181*, 687.
[29] S. Ninomiya, S. Adachi, *J. Appl. Phys.* **1995**, *78*, 1183.
[30] H.-J, Choi, J-K. Yang, H.-H. Park, *Thin Solid Films* **2006**, *494*, 207.
[31] A. L. Falk, F. H. L. Koppens, C. L. Yu, K. Kang, N. de Leon Snapp, A. V. Akimov, M. Jo, M. D. Lukin, H. Park, *H. Nature Photon.* **2009**, *5*, 475.
[32] I. P. Radko, S. I. Bozhevolnyi, G. Brucoli, L. Martin-Moreno, F. J. Garcia-Vidal, A. Boltasseva, *Phys. Rev. B* **2008**, *78*, 115115.
[33] S. A. Maier, *Plasmonics*,Springer, Berlin **2007**.
[34] J. Homola, *Surface Plasmon Resonance Based Sensors*, Springer, Berlin **2006**.
[35] W. Qingqing, X. Gang, H. Gaorong, *J. Solid State Chem.* **2005**, *178*, 2680.
[36] W. M. Buttler, W. Muscheid, *Ann. Phys.* **1954**, *15*, 82.
[37] F. A. Kröger, G. Diemer, H. A. Klasens, *Phys. Rev.* **1956**, *103*, 279.
[38] Y. Gu, J. P. Romankiewicz, J. K. David, J. L. Lensch, L. J. Lauhon, E.-S. Kwak, T. W. Kwak, T. W. Odom, *J. Vac. Sci.Technol. B* **2006** *24* 2172.

Received: June 2, 2010
Published online: August 3, 2010

